OPEN

Gene Therapy (2015) **22,** 707–720

www.nature.com/gt

ORIGINAL ARTICLE

Lentivirus-induced 'Smart' dendritic cells: Pharmacodynamics and GMP-compliant production for immunotherapy against TRP2-positive melanoma

BS Sundarasetty[1,10], L Chan[2], D Darling[2], G Giunti[2], F Farzaneh[2], F Schenck[3], S Naundorf[4], K Kuehlcke[4], E Ruggiero[5], M Schmidt[5], C von Kalle[5], M Rothe[6,10], DSB Hoon[7], L Gerasch[1,10], C Figueiredo[8,10], U Koehl[9,10], R Blasczyk[8,10], R Gutzmer[3,11] and R Stripecke[1,10,11]

Monocyte-derived conventional dendritic cells (ConvDCs) loaded with melanoma antigens showed modest responses in clinical trials. Efficacy studies were hampered by difficulties in ConvDC manufacturing and low potency. Overcoming these issues, we demonstrated higher potency of lentiviral vector (LV)-programmed DCs. Monocytes were directly induced to self-differentiate into DCs (SmartDC-TRP2) upon transduction with a tricistronic LV encoding for cytokines (granulocyte macrophage colony stimulating factor (GM-CSF) and interleukin-4 (IL-4)) and a melanoma antigen (tyrosinase-related protein 2 (TRP2)). Here, SmartDC-TRP2 generated with monocytes from five advanced melanoma patients were tested in autologous DC:T cell stimulation assays, validating the activation of functional TRP2-specific cytotoxic T lymphocytes (CTLs) for all patients. We described methods compliant to good manufacturing practices (GMP) to produce LV and SmartDC-TRP2. Feasibility of monocyte transduction in a bag system and cryopreservation following a 24-h standard operating procedure were achieved. After thawing, 50% of the initial monocyte input was recovered and SmartDC-TRP2 self-differentiated *in vitro,* showing uniform expression of DC markers, detectable LV copies and a polyclonal LV integration pattern not biased to oncogenic loci. GMP-grade SmartDC-TRP2 expanded TRP2-specific autologous CTLs *in vitro*. These results demonstrated a simpler GMP-compliant method of manufacturing an effective individualized DC vaccine. Such DC vaccine, when in combination with checkpoint inhibition therapies, might provide higher specificity against melanoma.

Gene Therapy (2015) **22,** 707–720; doi:10.1038/gt.2015.43

INTRODUCTION

Melanoma has rising incidence rates higher than any other malignancy. The field of treatment of metastatic melanoma is rapidly evolving at the moment with several targeted strategies in development.[1,2] Recent developments have considerably changed the standard of care for metastatic melanoma, such as for patients with metastatic melanomas harboring specific genetic mutations, that is, B-RAF^{V600} mutations. Trials with agents targeting these mutations such as Vemurafenib and Dabrafenib have shown objective responses and causing tumor regression in more than 50% of melanoma patients.[3,4] Despite these improvements, clinical responses are short term and tumor resistance to these molecular-targeted drugs is a common event. Therefore, other treatment options that provide long-lasting tumor control are warranted.

Melanoma is an immunogenic tumor, and thus a variety of immunotherapies have been explored to drive immune responses that are capable of long-term tumor control. Ipilimumab was recently approved as the first immune checkpoint inhibitor for the treatment of metastatic melanoma. Ipilimumab binds to CTLA-4, and therefore blocks a negative feedback mechanism that physiologically limits T-cell activation. By blocking this pathway, T cells stay activated, which results in a sustained and often long-term anti-tumor immune response in ~20% of patients.[5] The use of this agent in the adjuvant setting is currently investigated in a clinical placebo-controlled trial in stage III melanoma patients after complete resection of regional lymph node (LN) metastases. Unfortunately, strong off-target autoimmune side effects are regularly observed during ipilimumab therapy.[6] PD-1 has been explored as another immune checkpoint in melanoma, and two PD-1 blocking antibodies (pembrolizumab and nivolumab) have been recently registered by the Food and Drug Administration for the treatment of ipilimumab-refractory metastatic melanoma patients.[7–9] In addition, adoptive T-cell therapies are being developed in clinical trials with T-cell receptors and chimeric antigen receptors against a variety of melanoma-associated antigens and surface molecules expressed in melanoma, respectively.[10] Although immune responses generated by these engineered T cells are likely to be fast and potent, issues regarding tumor specificity and toxicity can lead to therapeutic risks.

[1]Department of Hematology, Hemostasis, Oncology and Stem Cell Transplantation, Hannover Medical School, Hannover, Germany; [2]Department of Hematological Medicine, Cell and Gene Therapy at King's, The Rayne Institute, King's College London, London, UK; [3]Department of Dermatology and Allergy, Skin Cancer Center Hannover, Hannover Medical School, Hannover, Germany; [4]EUFETS GmbH, Idar-Oberstein, Heidelberg, Germany; [5]Division of Translational Oncology, National Center for Tumor Diseases, Heidelberg, Germany; [6]Department of Experimental Hematology, Hannover, Germany; [7]John Wayne Cancer Institute, Santa Monica, CA, USA; [8]Department of Transfusion Medicine, Hannover Medical School, Hannover, Germany and [9]Institute for Cell Therapeutics and GMP core facility IFB-Tx, Hannover Medical School, Hannover, Germany. Correspondence: Professor Dr R Stripecke, Department of Hematology, Hemostasis, Oncology and Stem Cell Transplantation, Hannover Medical School, Hans Borst Zentrum, Carl Neuberg Strasse 1, Building J11, Floor 02, Room 6100, Hannover D-30625, Germany.
E-mail: stripecke.renata@mh-hannover.de
[10]Excellence Cluster REBIRTH.
[11]Co-senior authors.
Received 13 February 2015; accepted 23 March 2015; accepted article preview online 28 April 2015; advance online publication, 28 May 2015

On the other hand, numerous clinical trials have been carried out assessing the ability of adaptive immunotherapy using *ex vivo* generated conventional dendritic cells (ConvDCs) in the treatment of melanoma. DC vaccines are well tolerated and no toxicity was reported. Clinical trials with DC vaccines loaded with peptides demonstrated complete responses in 3%, partial response in 6% and stable disease in 21% of the patients tested.[11] However, DC clinical trials were compromised by several limitations in their production methods: high costs, poor consistency, and low viability of the *ex vivo* generated DCs loaded externally with antigens.[12] Although monocyte-derived DCs can be routinely produced *ex vivo* in the presence of recombinant cytokines and maturation factors, their migration from the immunization sites to lymph nodes was limited,[13] making this a major weakness in past DC vaccination studies. Moreover, major histocompatibility complex class I restricted peptide loading onto DC vaccines may be insufficient in generating broad immunological responses for significant clinical benefits.[14,15] In light of these reports, several clinical trials have been engaged in loading DCs with full-length melanoma-associated antigens,[16] co-culturing DCs with tumor lysates and mRNA transfection into the DCs for an optimal antigen delivery.[17]

Interestingly, DCs transfected with *in vitro* transcribed mRNAs have shown that the DC therapies have been feasible, safe and induce melanoma-specific immunological responses. DCs transfected with a mixture of RNAs encoding for stimulatory ligands and melanoma-associated antigens led to 30% overall survival rates in advanced pretreated unresectable melanoma patients (stage IIIC or IV) in the absence of additional melanoma treatments.[18] Recent phase I clinical trial results obtained from a single-arm, small patient study with a number of different mRNA modified DC therapies (including combination with interferon-α-2b (IFN-α-2b) adjuvant therapy) following the resection of melanoma metastases resulted in 2 and 4 year overall survival rates of 93% and 70%, respectively.[19] In this trial, overall survival was improved in the absence of a significant improvement in progression-free survival and therefore, encouraging, but no definitive conclusions could be drawn. Overall, mRNA delivery systems suffered from the instability of gene expression in electroporated DCs (that might be not highly viable *in vivo*). Moreover, DC vaccines transfected with mRNAs were less effective in animal models than more persistent gene delivery systems such as lentiviral vector (LV)-transduced DCs.[21]

Thus, clinical trials showing genetically modified DCs by various viral vectors (such as fowlpox, vaccinia and adenovirus vectors) expressing melanoma antigens were reported.[20] However, these vector systems had poor gene delivery efficiency, were cytotoxic to DCs or stimulated T cells responses against co-expressed viral proteins. Thus, in recent years, development of LVs has boomed for gene transfer and vaccination studies as they can infect non-proliferating cells, have low immunogenicity, can carry large amounts of transgenic cargo (up to 7 Kb) and lead to persistent transgene expression.[22] LV technologies have been shown safe in animal models and clinical trials for cancer immunotherapy using T cells engineered with chimeric antigen receptor,[23] gene therapy of adrenoleukodistrophy[24] and Wiskott Aldrich Syndrome.[25]

We have developed an innovative method for bio-engineering DC by genetic reprogramming of DC precursors.[26] *LV* gene co-transfer of granulocyte macrophage colony stimulating factor (GM-CSF) and interleukin (IL)-4 into hematopoietic precursors generated 'Self-differentiated Myeloid-derived Antigen-presenting-cells Reactive against Tumors-DC' ('SmartDC').[27,28] We showed that bone marrow precursor cells obtained from immune competent C57BL/6 mice or human $CD14^+$ monocytes transduced overnight with combinations of LVs co-expressing GM-CSF/IL-4 and a melanoma self-antigen (tyrosinase-related protein 2, TRP2) could be used directly after transduction as vaccines applied subcutaneously.[27,29] The innovation of this approach was that the injected cells engrafted, were highly viable and self-differentiated effectively into DC *in situ*. Histological and optical imaging analyses showed that SmartDC-TRP2 effectively migrated from the injection site to local draining lymph nodes of C57BL/6 mice, where they persisted for a few weeks, resulting into dramatic expansion of T cells and anti-melanoma responses.[26,29]

We therefore advanced the SmartDC concept for translation into clinical trials. In previous work, we reported a tricisitronic LV design for combined co-expression of human or mouse GM-CSF, IL-4 and TRP2 genes.[27] Potency of mouse SmartDC-TRP2 was shown in the homologous melanoma mouse model, whereas high viability of the cryopreserved human SmartDC-TRP2 product was confirmed in a xenogeneic mouse model by optical bioluminescence analyses.[27] We also showed proof-of-principle for a large-scale method of human SmartDC-TRP2 generation.[27] Here, we addressed key additional requirements for clinical development of SmartDC-TRP2. We demonstrate that T cells obtained from five advanced melanoma patients attained TRP2-specific functional cytotoxic T lymphocyte (CTL) responses after *in vitro* expansion with autologous SmartDC-TRP2. We also show proof-of-concept for good manufacturing practice (GMP)-compliant manufacturing and cryopreservation of SmartDC-TRP2, resulting into a thawed product with the expected quality control specification. The results obtained herein pave way for the future clinical trials toward immunotherapy of malignant melanoma patients with personalized SmartDC-TRP2 vaccines for adaptive melanoma-specific responses that might be eventually combined with checkpoint inhibitors in order to provide higher specificity against melanoma.

Figure 1. Pre-clinical validation of SmartDC-TRP2 in melanoma patients ($n = 5$). Human SmartDC-TRP2 generated from $CD14^+$ monocytes from melanoma patients show DC immunophenotye and are potential stimulators of T cells. $CD14^+$ monocytes were isolated from PBMNCs of melanoma patients, preconditioned with cytokines for 8 h and transduced with 2.5 μg p24 equivalents of LV-G242T for 16 h. Post transduction, cells were washed and cultured for 7 days in medium without cytokines. (**a**) Tricistronic LV used for generating the SmartDC-TRP2 showing the transgenes and 2 A elements. (**b**) Representative example of immunophenotypic analyses performed on day 7 SmartDC and SmartDC-TRP2. Filled and unfilled histograms indicate FACS analyses with isotype control or relevant mAbs; numbers indicate percentages of positive cells. (**c**) Immunophenotypic analyses of SmartDC-TRP2 generated from five independent melanoma patients. Bar graphs indicate percentage positive cells. (**d**) Secreted cytokines in supernatants of SmartDC and SmartDC-TRP2 analyzed at day 7. White bars indicate GM-CSF and black bars indicate IL-4. (**e**) Baseline TRP2 reactivity analyzed by quantifying the $CD8^+$ T cells reactive against TRP2 tetramers: $TRP2_{180\text{-}188}$ and $TRP2_{360\text{-}368}$ in five different melanoma patients used in the study. An irrelevant tetramer was used as negative control. (**f**) SmartDC, SmartDC/pep or SmartDC-TRP2 were used in stimulation of autologous $CD8^+$ T cells from the respective melanoma patients. Relative fold expansion of T cells per group determined with trypan blue exclusion staining (relative to T-cell input). Line graph indicate the average values of independent experiments and error bars indicate mean ± s.e.m. $^*P < 0.05$. (**g**) IFN-γ ELISPOT analyses after two stimulations. 30 000 CD8+ T cells were co-cultured in the presence of KA2 cells or KA2 cells endogenously expressing TRP2 (KA2/TRP2) on IFN-γ coated ELISPOT plate. T cells without any were used as controls. Average number of spots from duplicate wells was quantified. Histograms represent average number of spots from pooled microculture wells ($n = 3$) per experimental condition. Bar graphs indicate average values of experiments performed and error bars indicate mean ± s.e.m. $^{***}P < 0.001$ and $^{**}P < 0.01$. (**h**) Analyses of TRP2-specificity by tetramer analyses. Dots indicate the frequencies of non-specific (control tetramer, circles), $TRP2_{180\text{-}188}$ (squares) and $TRP2_{360\text{-}368}$ (triangles) reactive $CD8^+$ T cells after three cycles of stimulation with SmartDC, SmartDC/pep or SmartDC-TRP2. Results for three melanoma patients are shown.

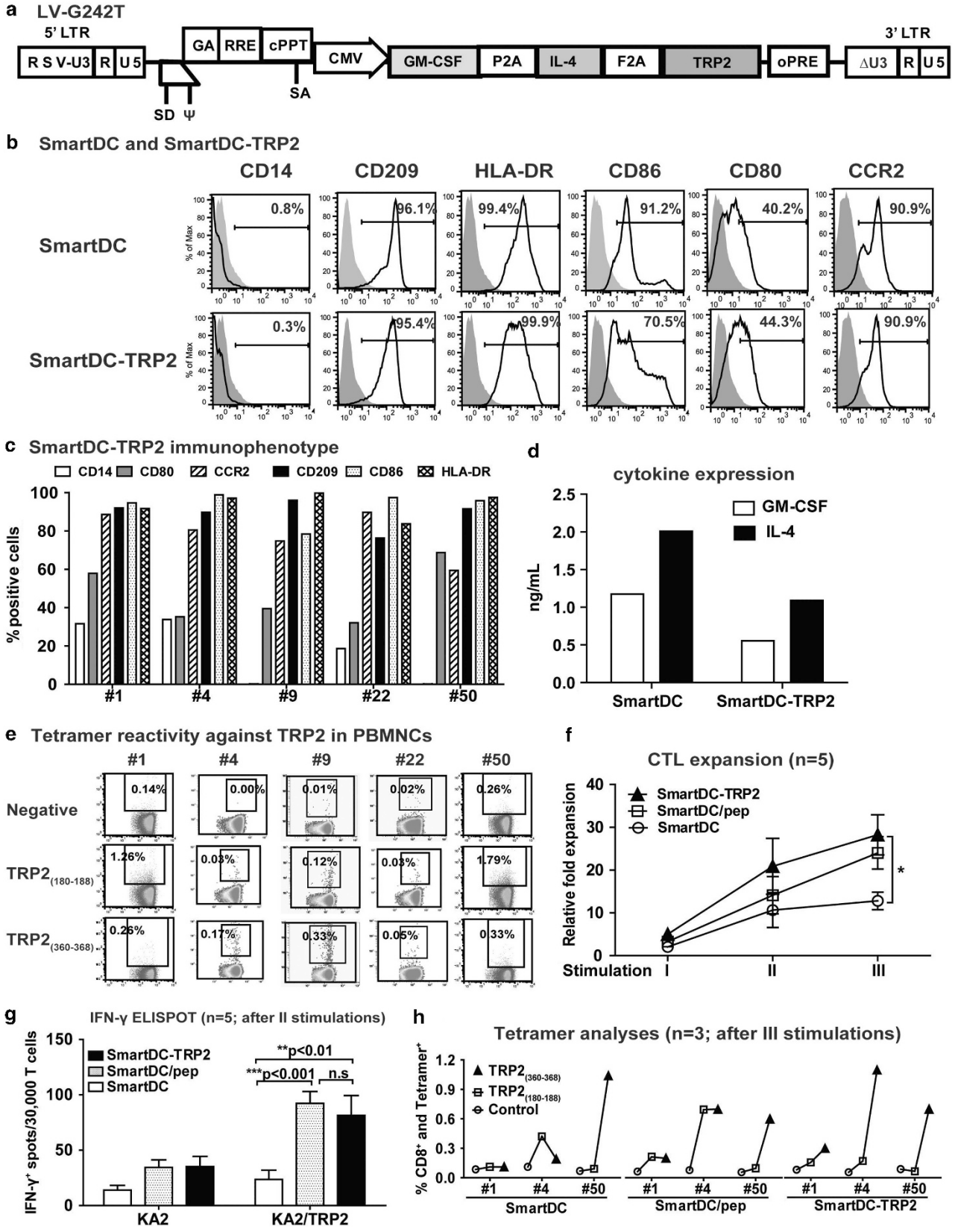

RESULTS

Generation and potency testing of SmartDC-TRP2 from melanoma patients

The tricistronic LV-G242T (Figure 1a) co-expressing GM-CSF, IL-4 and TRP2 interspaced with 2A elements was used to transduce $CD14^+$ monocytes isolated from five melanoma patients. As a control group, we included transduction of monocytes with LV-G24 vector for production of 'empty' SmartDC (that is, not expressing the antigen). The immunophenotypes of SmartDC-TRP2 and SmartDC 7 days after transduction and *in vitro* culture were comparable for all patients (Figure 1b, representative data). SmartDC-TRP2 productions resulted in cells with low frequencies of the monocytic marker CD14 and high frequencies of cells expressing the DC markers CD80, CCR2, CD209, CD86 and HLA-DR (Figure 1c). Cell supernatants were collected on day 7 of culture for detection of transgenic GM-CSF and IL-4 cytokines (Figure 1d). As CTLs reactive against TRP2 were previously identified in tumors of melanoma patients,[30] we therefore analyzed the peripheral blood samples of melanoma patients in our study for the presence of baseline TRP2-specific CTLs by tetramer analyses of $TRP2_{180\text{-}188}$ and $TRP2_{360\text{-}368}$ HLA-A*02:01-restricted epitopes (Figure 1e). Staining with tetramers binding to an irrelevant epitope was run as negative control. Three of the melanoma patients showed low tetramer reactivity against $TRP2_{180\text{-}188}$ ($< 0.1\%$ tetramer positive), whereas two patients showed 1.3 and 1.8% CTL reactivity against $TRP2_{180\text{-}188}$ (Figure 1e). Tetramer reactivity against $TRP2_{360\text{-}368}$ was lower, with CTL frequency in average 0.2% (Figure 1e). In order to evaluate the *in vitro* activation of autologous CTLs, 'empty' SmartDC, SmartDC/pep or SmartDC-TRP2 were co-cultured with $CD8^+$ T cells for up to three rounds of stimulation (Figure 1f). SmartDC-TRP2 stimulated the highest expansion of CTLs after three rounds of stimulations and was significantly higher than SmartDC (28 fold vs 10 fold; $P < 0.05$, relative to the T cell input). SmartDC/pep induced slightly lower T cell expansion (21 fold) compared to SmartDC-TRP2 (Figure 1f, Table 1). The expanded CTLs were subsequently seeded on IFN-γ coated plates overnight with target KA2 'empty' cells or KA2 cells expressing full-length TRP2 (KA2/TRP2). CTLs harvested after two rounds of stimulations with SmartDC-TRP2 or SmartDC/pep showed significantly higher reactivity against KA2/TRP2 than CTLs expanded with SmartDC (3.5-fold; $^{**}P < 0.01$ and 4-fold; $^{***}P < 0.001$, respectively; Figure 1g). *In vitro* expanded CTLs were analyzed for the specificity against TRP2 epitopes by tetramer analyses. Overall, a modest reactivity against $TRP2_{180\text{-}188}$ was observed for all CTL groups (Figure 1h). A trend for higher CTL reactivity against $TRP2_{360\text{-}368}$ was observed after expansion of T cells with SmartDC/pep or with SmartDC-TRP2 than with 'empty' SmartDC (Figure 1h, Table 1). Nevertheless, we could not establish a firm correlation between the frequencies of TRP2-reactive CTLs at baseline for each patient detected by tetramers and after *in vitro* expansion. It is possible that CTLs reacting against other epitopes in TRP2 may be preferentially expanded. In summary, comparing the effects of SmartDC-TRP2 (loaded with TRP2 endogenously) or SmartDC/pep (loaded with antigens on the cell surface) versus 'empty' SmartDC for the different analyses, the IFN-γ ELISPOT assay showed superior consistency for quantification of anti-TRP2-specific reactivity than analyses of T-cell expansion or tetramer reactivity (Table 1).

CTLs expanded with SmartDC-TRP2 lyse TRP2-positive cells *in vitro*

We developed an assay to evaluate the potency of *ex vivo* expanded TRP2-reactive CTLs regarding their capacity to specifically lyse HLA-A*02:01-positive targets expressing TRP2 (Figure 2a). KA2, KA2/TRP2 and FEMX-I (a TRP2-positive human malignant melanoma cell line originating from a lymph node metastasis) cells were used as targets (Figure 2b). All cell lines, including FEMX-1, were uniformly labeled with CFSE (Figure 2c). Upon exposure to the CTLs, cell lysis could be followed by flow cytometry as decreased frequencies of CD8 – /CFSE-labeled viable cells (Figure 2c). At various effector to target ratios (E:T ratios), only 10–40% of the KA2 target cells (exposed to CTLs expanded with all the three types of DCs) were lysed (Figure 2d). When KA2/TRP2 were used as targets, significantly higher lysis was produced by CTLs expanded with SmartDC-TRP2 and used at higher E:T ratios (9:1 and 27:1, Figure 2e) than CTLs expanded with SmartDC. When FEMX-I cells were used as targets, the cytotoxicity caused by CTLs expanded with SmartDC-TRP2 was significantly higher for all E:T ratios tested (Figure 2f). These specific immune response assays indicated that CTLs reactive against TRP2 are present in peripheral blood mononuclear cells of melanoma patients that can be activated *in vitro* with SmartDC-TRP2, in an antigen-specific manner, to recognize and kill melanoma.

Production of LV-G242T and SmartDC-TRP2 under GMP-compliant conditions

We assessed the proof-of-concept feasibility of SmartDC-TRP2 production entirely under GMP-compliant conditions. We validated the upstream and downstream processes and established standard-operating-protocols for the production of LV-G242T. High-purity supercoiled plasmids were used for transfection of 293 T cells in layer flasks (Figure 3a). After transfection, viral supernatants were harvested and subjected to downstream purification (benzonase treatment, filtration, chromatographic purification, centrifugation, filling and storage. The entire process was performed in clean rooms). Total LV-G242T content was determined by p24 ELISA for each processing step (Figure 4a). The final LV product corresponded to 148.5 µg p24 equivalent or 2.8×10^9 infective units (determined by PCR). SmartDC-TRP2 production under GMP-like compliant conditions (that is, outside the clean rooms but with GMP-grade material) was subsequently

Table 1. Comparisons between *in vitro* assay analyses

Patient number	*IFN- γ ELISPOT after II stimulations*			*$CD8^+$ T-cell expansion after III stimulations*			*$TRP2_{360\text{-}368}$ tetramer (% tetramer$^+$ in $CD3^+/CD8^+$ cells)*		
	SmartDC	*SmartDC/pep*	*SmartDC-TRP2*	*SmartDC*	*SmartDC/pep*	*SmartDC-TRP2*	*SmartDC*	*SmartDC/pep*	*SmartDC-TRP2*
#1	14.0	94.0	60.0	9.7	14.0	14.5	0.1	0.2	0.3
#4	16.0	84.0	86.0	17.1	22.3	36.7	0.2	0.7	1.1
#9	40.0	105.0	105.0	18.0	33.3	40.9	NA	NA	NA
#22	63.0	103.0	145.0	8.4	32.1	25.2	NA	NA	NA
#50	6.0	54.0	35.0	10.4	18.4	22.5	1.0	0.6	0.7
Mean±s.e.m.	27.8±12.1	88.0±10.7	86.8±17.9	12.7±1.8	24.0±3.4	28.0±4.3	0.4±0.23	0.5±0.12	0.7±0.18
Fold change vs SmartDC	—	3.2	3.1	—	1.9	2.2	—	1.2	1.8

Abbreviations: CTL, cytotoxic T lymphocyte; IFN-α, interferon-α; PBMNC, peripheral blood mononuclear cell; SmartDC, self-differentiated myeloid-derived antigen-presenting-cells reactive against tumors-dendritic cell; TRP2, tyrosinase-related protein 2. SmartDC-TRP2 potency assays performed with PBMNCs obtained from advanced melanoma patients. IFN-γ ELISPOT, T-cell expansion and CTL reactivity by tetramer ($TRP2_{360\text{-}368}$) analyses obtained for melanoma patients. Fold increase was calculated for SmartDCs expressing or loaded with the TRP2 antigen versus 'empty' SmartDC used for CTL expansion *in vitro*.

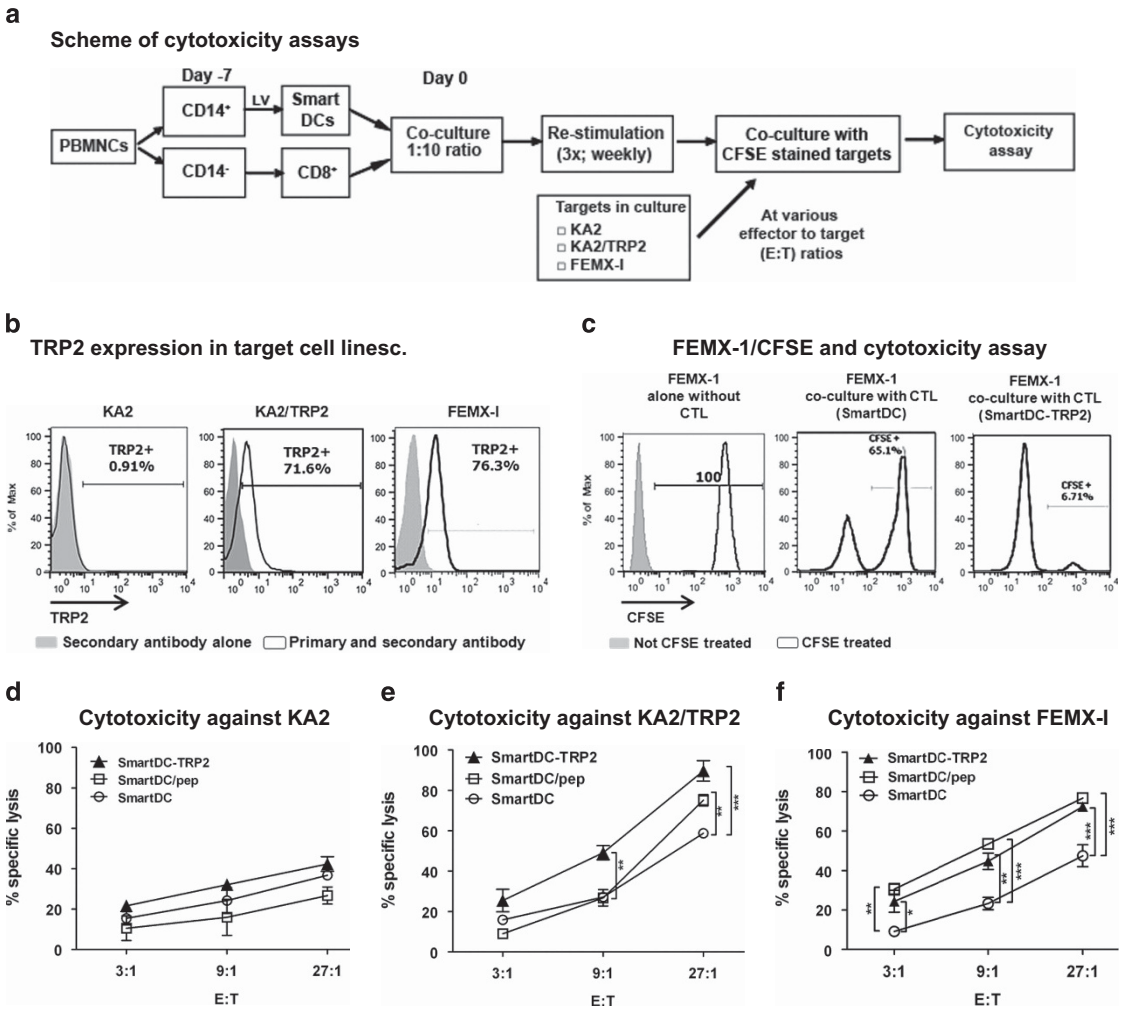

Figure 2. Pre-clinical validation of SmartDC-TRP2 potency generated from melanoma patients. CTLs stimulated with SmartDC or SmartDC/pep or SmartDC-TRP2 were analyzed for their ability to specifically lyse the target cells expressing TRP2. CTLs were co-cultured with TRP2 expressing KA2/TRP2 or FEMX-I cells at various effector to target (E:T) ratios and the cytotoxic ability was determined by CFSE-based assay. (**a**) Scheme of cytotoxicity assays. (**b**) TRP2 expression in KA2, KA2/TRP2 and FEMX-I target cells analyzed by intracellular staining. Filled and unfilled histograms indicate FACS analyses with isotype control or relevant mAbs; numbers indicate percentages of positive cells. (**c**) CFSE staining of FEMX-I targets used in the cytotoxicity assays. CFSE staining of FEMX-I targets before co-culture with the effector cells in the cytotoxicity assay and CFSE staining of FEMX-I targets after co-culture with CTL generated with SmartDC and CTL generated with SmartDC-TRP2. The right peak in the histograms show the live $CFSE^+$ targets after the cytotoxicity. Filled histogram in the first panel indicates isotype control for CFSE staining. (**d–f**) CFSE-based cytotoxicity assays. The line graph shows the percentage-specific lyses of T cells obtained from the microcultures of melanoma patients ($n=3$). The data represents the average of triplicate wells performed with cells obtained from microcultures after three stimulations. (**d**) KA2 as targets, (**e**) KA2/TRP2 as targets and (**f**) FEMX-I as targets. T cells stimulated with SmartDC without any antigen is shown in open circles; T cells stimulated with SmartDC-TRP2 are shown in black triangles. Error bars indicate mean ± s.e.m.; $^{***}P<0.001$, $^{**}P<0.01$ and $^{*}P<0.05$.

performed. The leukapheresis product obtained from a HLA-A*02:01 positive donor was transported under controlled conditions to the GMP facility. The entire cell handling (leukapheresis, $CD14^+$ isolation, cytokine preconditioning, transduction, wash and cryopreservation) was completed in a total of 3 days, from which the gene transfer required 24 h of processing (Figure 3b). Quality control analyses were included after each step of the process to assess viable cell recovery (Figure 4a). SmartDC-TRP2 were cryopreserved at a density of $2\times10^6\,ml^{-1}$ per vial and were maintained cryopreserved for at least 10 days prior to thaw and final quality control.

Characterization of the genetically modified cell product after *in vitro* culture

Analytical methods were applied for independent triplicates in order to demonstrate the consistent viability, morphology, self-differentiation, expression of transgenic cytokines and endogenously upregulated cytokines after thawing and *ex vivo* culture. Cryopreserved monocytes from the same $CD14^+$ selection used for SmartDC-TRP2 production were thawed and used as mock controls. As an additional control group, monocytes were thawed and ConvDCs were prepared in the research laboratory (culture with GM-CSF and IL-4). After 7 days of culture, 36–48% and 30–38% recovery was obtained for SmartDC-TRP2 (maintained in CellGro) and ConvDCs (maintained in CellGro plus cytokines) relative to thawed input, respectively (Figure 4c). Thus, GM-CSF and IL-4 gene transfer resulted in higher cell recovery on day 7 than culture with exogenous cytokine treatment, whereas only 11–14% of monocytes maintained in CellGro were recovered after 7 days (Figure 4c). SmartDC-TRP2 analyzed immediately after thaw showed high viability (>90% $7AAD^{neg}$) and purity (>90% $CD45^+$ and $CD14^+$ no T, B and natural killer cells; Figure 4d). After *in vitro*

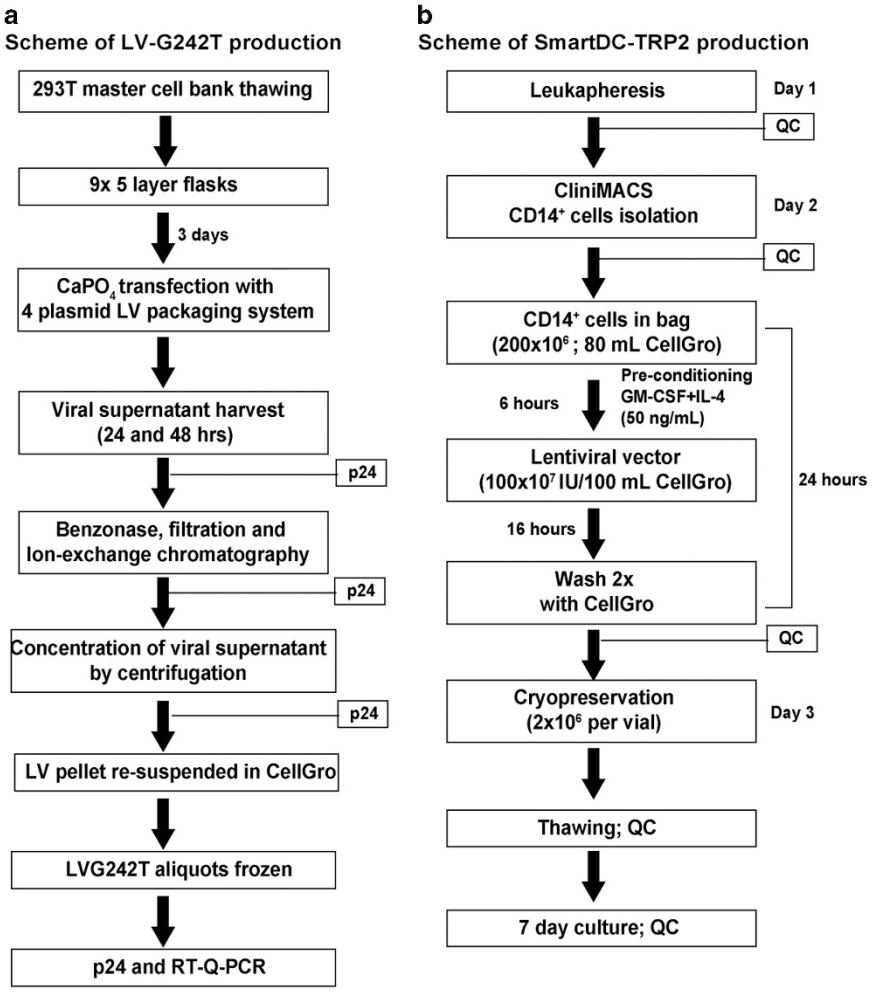

Figure 3. Standardized production of LV-G242T and SmartDC-TRP2 under GMP-compliant conditions: up-scaling and recovery. (**a**) Schematic representation of pilot batch of the lentiviral vector production performed under GMP-compliant conditions. (**b**) Schematic flow diagram representing the production of one pilot batch of SmartDC-TRP2 generation under GMP-like conditions.

culture, SmartDC-TRP2 showed typical DC morphology (Figure 4e) and immune phenotypic features (downregulation of CD14; high expression of DC markers CD209, CD86 and HLA-DR; Figure 4f). Significantly higher concentrations of GM-CSF (17.7 pg ml^{-1}), IL-4 (22.3 pg ml^{-1}), monocyte chemoattractant protein-I (1938.7 pg ml^{-1}) and interleukin-8 (IL-8) (2707.1 pg ml^{-1}) were obtained for SmartDC-TRP2 than in monocyte culture supernatants harvested on day 7 (Figures 4g and h).

Analyses of vector titer and genomic integration of LV sequences in SmartDC-TRP2

DNA was isolated from SmartDC-TRP2 maintained in culture for 7 days and mock monocytes were used as baseline controls. Detectable LV copies were obtained in transduced monocytes at 1.66 copies per cell (mock monocyte controls: 0.003 copies per cell; Figure 5a). As LVs are actively being pursued in clinical trials, risk concerns regarding insertional mutagenesis require comprehensive characterization of the product. Although DCs are post-mitotic and non-replicating cells, a biased integration pattern in a potentially oncogenic locus could predispose to insertional mutagenesis and genotoxic effects. Therefore, LV integration pattern in genomic DNA obtained from day 7 SmartDC-TRP2 was analyzed by linear amplification mediated-PCR (LAM-PCR) and next-generation sequencing and the clonal frequencies were monitored with a high-throughput integration site (IS) analysis.[31] The number of total vector sequences that could be retrieved for the SmartDC-TRP2 were in the order of 10^4, whereas after applying the filtering methods, the detectable number of unique IS was 159 (46-fold reduction; Figure 5b). The integration pattern was highly polyclonal and the 10 most frequent identified gene loci were discordant and did not occur near oncogenes (Figure 5c). LV integrations were not found in chromosome Y. For all other chromosomes, integration frequencies were roughly correlated with chromosome size (Figure 5c). As expected, LV integrated sequences were found in higher frequency in genes than in regions upstream of the transcription start site (Figure 5d). Overall, these analyses confirmed previous observations that LV integrations are random showing a polyclonal non-biased integration profile not matching a known biased integration sequences assigned for gamma-retroviral genotoxicity, such as LMO2.[32]

Potency of GMP-grade SmartDC-TRP2

GMP-grade SmartDC-TRP2 cultured for 7 days were mixed with autologous CD8$^+$ T cells (DC 1: T cell 10 ratio) for up to three consecutive stimulation rounds (Figure 6a). Research-grade

'empty' SmartDC and SmartDC/pep generated from the same CD14$^+$ selection were used as negative and positive controls, respectively. All co-cultures were set up in triplicates. Relative to T-cell input, SmartDC-TRP2 stimulated the highest expansion of T cells after three rounds of stimulations (20-fold), followed by SmartDC/pep (10-fold) and SmartDC (5-fold) (Figure 6b). For IFN-γ ELISPOT assay, T cells stimulated with DCs twice were co-cultured with target KA2 or KA2/TRP2. Relative to T cells expanded with

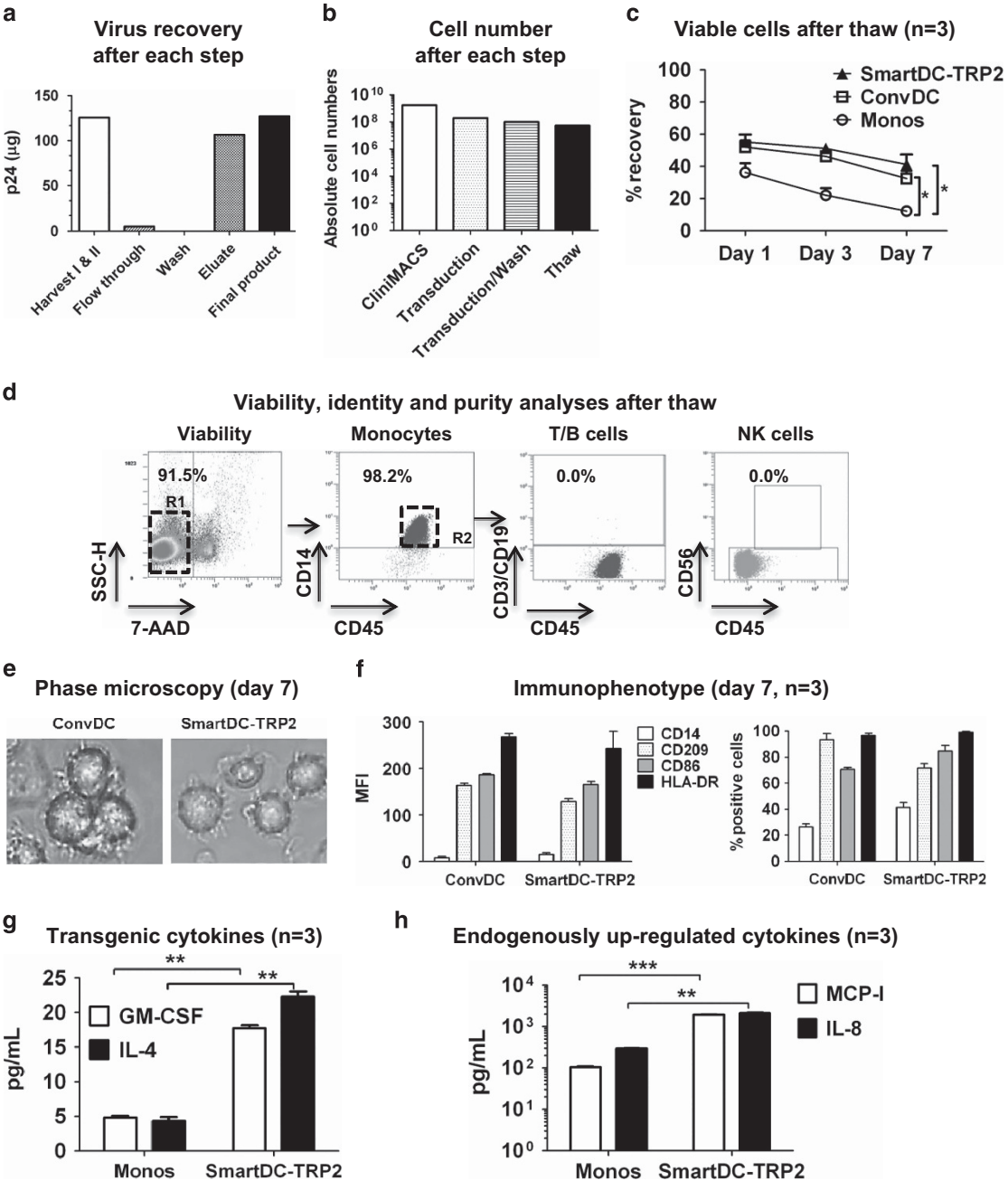

Figure 4. Characterization of SmartDC-TRP2 produced under GMP-compliant conditions. CD14$^+$ monocyte selection was performed by CliniMACS. 2×10^8 monocytes were transduced in bags with 1×10^9 infectious particles at an multiplicity of infection (MOI) of 5. Transduced monocytes were washed and cryopreserved. SmartDC-TRP2 produced under GMP were thawed, cultured *in vitro* and analyzed on days 1, 3 and 7. Characterization was aimed at specifying markers of DC differentiation and potency. (**a**) LV-G242T recovery after each step of production process. (**b**) CD14$^+$ cell recovery as viable cell numbers after each step of production process and after thaw (extrapolated). (**c**) Percentage recovery of viable cells (determined by trypan blue dye exclusion) on days 1, 3 and 7 after culture in medium without exogenous addition of cytokines ($n=3$). Line graph indicate average values obtained from three independent experiments. Error bars indicate mean ± s.e.m. *$P<0.05$. (**d**) Representative example of QC and batch release criteria for one GMP-like batch, showing high viability, purity and expected monocyte characteristics of the product after thawing. (**e**) Phase microscopy of SmartDC-TRP2 showing typical DC morphology on day 7 of *in vitro* culture, comparable to ConvDC cultured in the presence of cytokines. (**f**) Immunophenotypic analyses as percentage positive and mean fluorescent intensity (MFI). Histogram bars represent average values obtained from three independent experiments. Error bars indicate mean ± s.e.m. (**g**) Concentration of GM-CSF and IL-4 in cell supernatants harvested on day 7 after thaw (pg ml^{-1}). (**h**) Concentration of endogenously upregulated MCP-1 and IL-8 (pg ml^{-1}). Data represents the average of three independent runs. Bar graphs indicate mean and error bars indicate mean ± s.e.m. **$P<0.01$; ***$P<0.001$.

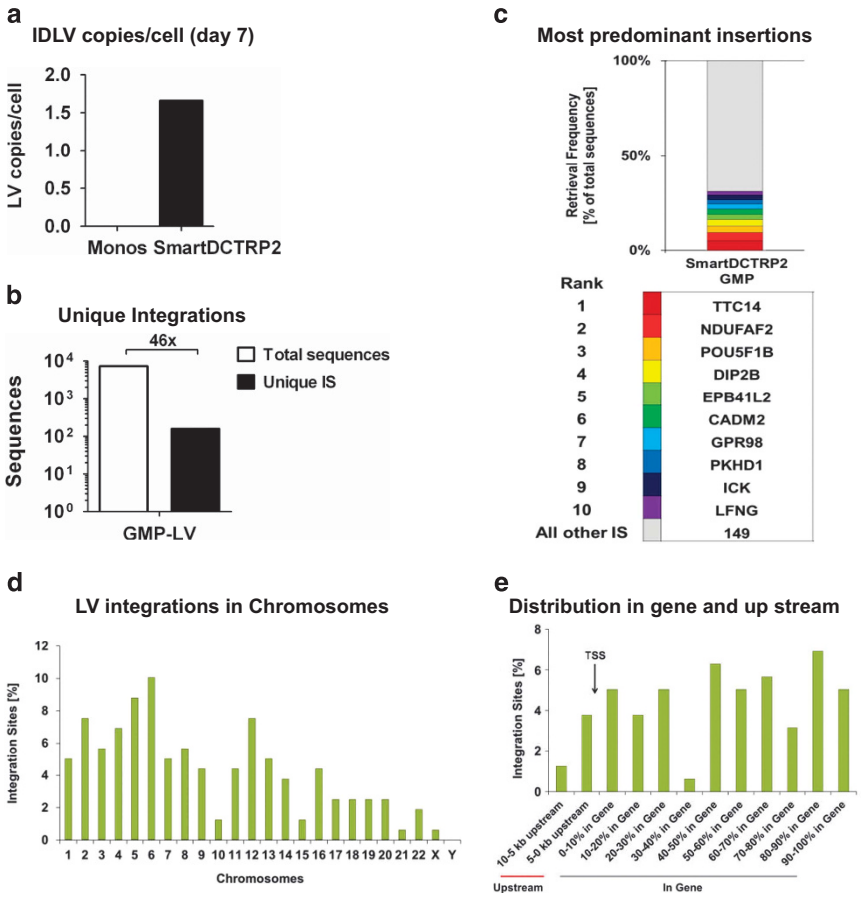

Figure 5. Characterization of LV-G242T and integration site analyses in SmartDC-TRP2. (**a**) Transduced monocytes were thawed and cultured *in vitro* for 7 days without exogenous addition of cytokines. On day 7, cells were harvested and analyzed by RT-q-PCR and integrated LV copy numbers were determined (expressed as LV copies per cell). Monocytes were used as controls. (**b**) Total matched sequences and unique integration sites (IS) analyses performed after LAM-PCR with the tDNA extracted from SmartDC-TRP2 (day 7) followed by NGS. Fold reduction from the total matched sequences to IS is indicated. (**c**) 10 most predominant clones in SmartDC-TRP2. Colored columns represent retrieval frequency as percentage of total sequences. Larger colored bars represent higher frequencies of integration sites clustering in the proximity of that gene. Lower panel: ranking of the 10 most predominant clones with their corresponding color code and gene ID. (**d**) Frequency of integrations per chromosome for the lot of GMP-compliant SmartDC-TRP2. (**e**) Distribution of integrations upstream of transcription start sites (TSS; arrow) or in genes for research GMP-compliant batch of SmartDC-TRP2.

'empty' SmartDC, significantly higher reactivity against KA2/TRP2 cells was observed for T cells stimulated with SmartDC-TRP2 (11-fold; $^{****}P < 0.0001$) or with SmartDC/pep (3-fold; $^{**}P < 0.01$; Figure 6c). CTLs expanded after three rounds of stimulation were analyzed for their ability to lyse target cells using a lactate dehydrogenase-based cytotoxicity assay. Expanded T cells showed low reactivity ($< 5\%$ lyses) against the negative control KA2 targets at different E:T ratios (Figure 6d). At the highest E:T ratio (27:1), T cells stimulated with SmartDC-TRP2 or SmartDC/pep and co-cultured with KA2/TRP2 cell resulted into ~30% cytotoxicity (10- and 8-fold higher than CTLs expanded with SmartDC, respectively (Figure 6e)). Thus, SmartDC-TRP2 produced under GMP-compliant conditions expanded T cells capable to specifically recognize and lyse TRP2-positive cell targets.

DISCUSSION

Several clinical and preclinical studies have pointed out that the optimal approach to control recurrent melanoma will likely be a combination of de-bulking strategies (surgery and systemic therapies) with adjuvant immune modulators and personalized immune therapy approaches. The current work results from further translational developments of the SmartDC technology previously tested with murine SmartDC derived from bone marrow unfractionated cells *in vivo* using the B16 melanoma model transplantable to C57BL/6 mice. We have previously shown in several publications that SmartDC-TRP2 consistently resulted into expansion of TRP2-specific $CD8^+$ T cells that induced B16 tumor protection or regression.[26,27,29] Mouse SmartDC were more viable (2–3 weeks) than ConvDCs produced with recombinant cytokines and actively migrated to adjacent inguinal lymph nodes. Other than sporadic vitiligo and alopecia, probably mediated due to abrogated immune tolerance for skin and hair follicle cells producing melanin, no other toxicities or malignancies were observed in mice maintained long term. Concurrently, we have also previously shown that human cryopreserved/thawed SmartDC-TRP2 marked with firefly luciferase were viable for 3–4 weeks after subcutaneous injection in Nod.Rag1$^{-/-}$.IL2rγ$^{-/-}$ mice with no toxic effects. Thus, these preclinical relevant *in vivo* models demonstrated efficacy and safety of SmartDC-TRP2 in stimulation of TRP2-specific CTLs.

We demonstrated previously that mouse SmartDC-TRP2 injected subcutaneously into C57BL/6 mice after a lethal B16 melanoma challenge significantly controlled tumor growth and delayed death, but long-term survivors were rare.[26,27,29] This could be explained by the explosive and immune suppressive behavior

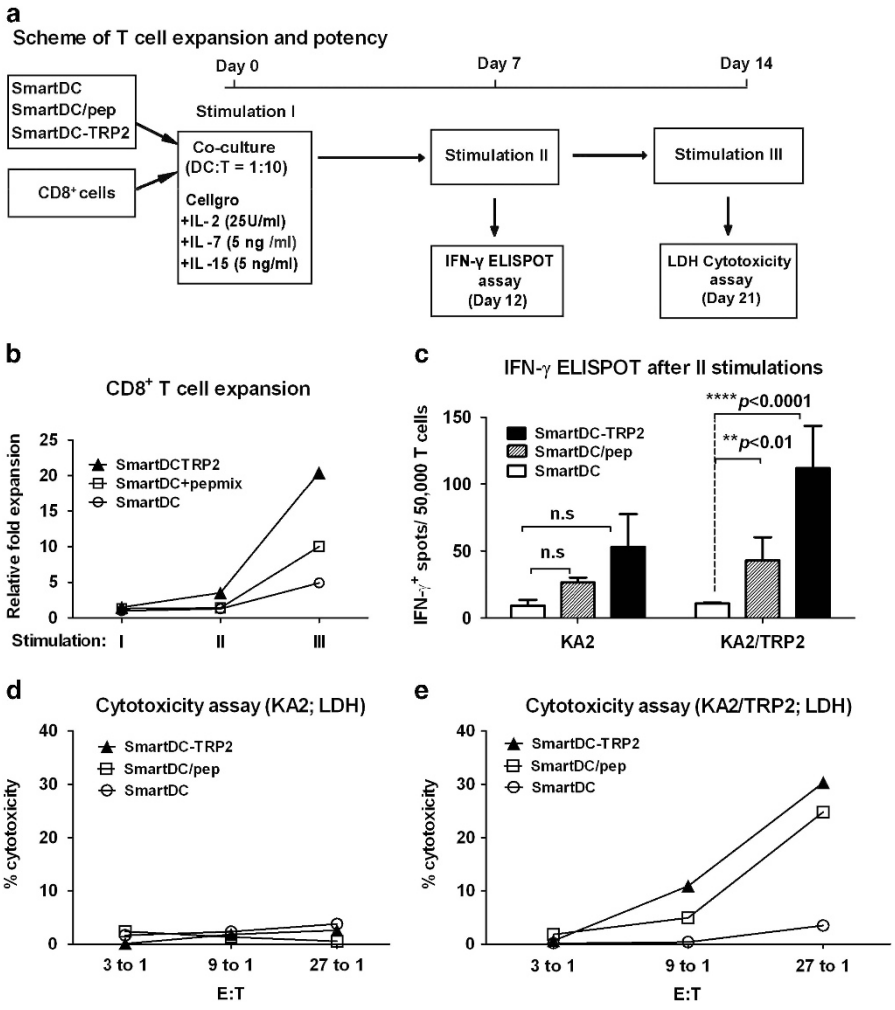

Figure 6. Characterization of SmartDC-TRP2 potency produced under GMP-compliant conditions. SmartDC-TRP2 thawed and cultured *in vitro* for 7 days were used in stimulation of autologous $CD8^+$ T cells. SmartDC and SmartDC loaded with TRP2 peptide mix were used as controls. CTLs were harvested after 7 days of co-culture with respective SmartDC groups and analyzed. Three rounds of stimulations were performed. (**a**) Scheme of T-cell stimulation, expansion and analyses. (**b**) Relative fold expansion of T cells per group determined with trypan blue exclusion staining (relative to T-cell input). Line graph indicate the average values of independent experiments and error bars indicate mean ± s.e.m. (**c**) IFN-γ ELISPOT analyses after two stimulations. 50 000 $CD8^+$ T cells were co-cultured in the presence of KA2 cells or KA2 cells endogenously expressing TRP2 (KA2/TRP2) on IFN-γ ELISPOT plates. Non-stimulated T cells were used as controls. Average number of spots from duplicate wells was quantified. Histograms represent average number of spots from pooled microculture wells ($n = 3$) per experimental condition. Bar graphs indicate average values of experiments performed and error bars indicate mean ± s.e.m. $^{****}P < 0.0001$ and $^{**}P < 0.01$. (**d** and **e**) Cytotoxicity assay based on LDH. T cells stimulated with SmartDC-TRP2 were co-cultured with (**d**) KA2 or (**e**) KA2/TRP2 targets at various effector to target (E:T) ratios. 8 h after the incubation, target cell lysis was determined by quantifying the LDH release in the respective wells. SmartDC and SmartDC loaded with TRP2 pepmix (SmartDC/pep) were used as controls. Percentage cytotoxicity was calculated by the following formula: % Cytotoxicity = (Experimental release-Effector spontaneous-Target spontaneous/Target maximum-Target spontaneous) × 100. Line graph indicate the values quantified from triplicate wells.

of the B16 melanoma model once it takes hold. Nevertheless, we observed in these studies, that the local LN became greatly enlarged, resulting in a massive accumulation of host DC and TRP2-reactive lymphocytes. High frequencies of CTL reactive against TRP2 were detectable in spleen and LN as measured by intracellular IFN-γ assays.[29] Here, we corroborate the findings with the human *in vitro* assays studies, showing that SmartDC-TRP2 generated from five advanced melanoma patients were highly potent in expanding CTL memory cells and inducing TRP2-specific lytic responses.

TRP2 (also known as dopachrome tautomerase) is a highly conserved trans-membrane enzyme involved in tyrosine metabolism, metabolic pathways and in melanogenesis.[33] TRP2 is expressed in normal (retina, melanocytes), pre-malignant tissues (nevi) and tumors (melanocytic or amelanocytic melanoma, retinoblastomas and glioblastomas). Melanoma cells show higher TRP2 expression than normal melanocytes, and TRP2 function has been linked with resistance of melanoma cells to chemotherapy and radiation treatments.[33] T-cell and humoral reactivity against TRP2 could be demonstrated in healthy and cancer patients, demonstrating that central tolerance for this antigen is not full, that is, TRP2-reactive T cells are not depleted from the repertoire and memory cells persist for immune surveillance.[34–36] This agrees with experimental systems such as transgenic mice developing disseminated melanoma showing high frequencies of effector memory $CD8^+$ T cells reactive against TRP2 at the phase of microscopic tumor load in lymph nodes.[37] In another transgenic mouse model recapitulating spontaneous melanoma, TRP2 has been used as a marker for assessing melanoma spread, remarkably revealing that melanoma disseminated in LN showed

upregulation of TRP2 expression.[38] Incidentally, TRP2 mRNA can also be detected by quantitative PCR in tumor lesions and sentinel LN of metastatic melanoma patients, demonstrating that the antigen expression in tumor cells is not downregulated in these key tissues, potentially enabling their recognition by CTLs.[39,40] Surprisingly, despite vast experimental and clinical evidence showing that non-mutated TRP2 is immunogenic, that TRP2 expression is maintained in melanoma spreading to LN and that TRP2-specific CTLs can be quite potent at eliminating melanoma, adoptive or adaptive immune therapies targeting TRP2 have not been explored clinically.

The understanding of the tumor/host interaction is unraveling with the clinical success and pitfalls of checkpoint blockers such as PD-1. One interesting proposed counter-acting mechanism to this therapy is the tumor adaptive immune resistance (that is, PD-L1 upregulation) in response to antigen-specific T-cell infiltration into melanoma tumors.[41] Quantification of CTL infiltrates in tumors or CTL expansion in sentinel LN are proposed to have predictive value with respect to tumor regression.[41] Therefore, if SmartDC-TRP2 can induce a broad and effective type-I IFN inflammatory CTLs able to accumulate in melanoma and LN metastases, the combination of this vaccine with PD-1 blockade will merit clinical investigation.

The field of melanoma immune therapy has recently focused on the discovery of class I-restricted neo-antigens, such that a highly personalized antigenic or adoptive CTL treatment could be administered. Yet, recognition of neo-antigens that arise due to mutations in melanoma by $CD4^+$ cells seems to be more frequent and relevant than previously anticipated.[42] Thus, presentation of the full-length TRP2 antigen by SmartDC-TRP2 can activate both CTL and helper responses. This could be ideally combined with immunization with peptides encompassing class I- and class II-restricted neo-antigens. This way, melanoma growth could be combated immunologically in two fronts: as a first multipotent and broad immunologic hit against the over-expressed self-antigen TRP2 in order to enhance type-I interferon inflammation in tumor and LN, and a second immunologic hit, specifically against mutated neo-antigens.

For these reasons, advancing toward innovative translational combinations of immune therapies is currently warranted to progress toward the next therapeutic level. At the same time, cellular or viral vaccines will require simple and consistent production method to facilitate multiple vaccination cycles and large clinical trials to answer questions of efficacy. Emphasizing these requirements, in this study we demonstrated that LV-G242T was readily successfully produced and purified in an academic GMP manufacturing facility. These data demonstrated that our LV production is comparable with the production methods that are now currently being used by biotech companies for use in clinical trials.[43,44] In addition, feasibility of the entire production and cryopreservation of the individualized SmartDC-TRP2 vaccine under GMP conditions was achieved in only 3 days. About 25% of the monocytes were recovered after transduction, wash, cryopreservation and thawing. Previous studies with conventional DC vaccines reported typically the use of 4×10^6 to 1×10^7 cells for vaccinations in order to induce relevant immune responses.[14,45,46] Thus, starting with 2.0×10^8 cells used for transduction, 5×10^7 viable cells after thawing would be enough to complete quality control requirements and to be used in prime/boost immunizations combined with checkpoint blockade therapies. The European Medical Agency requires rigorous characterization of the cell product prior to administration into patients. Therefore, SmartDC-TRP2 after thawing and *in vitro* culture were subjected to analyses of identity, potency and effects of gene transfer. Immediately after thawing, SmartDC-TRP2 corresponded to $>90\%$ pure $CD14^+$ monocytes, conforming to the identity of the cell type used for genetic manipulation. After 7 days of *in vitro* culture, SmartDC-TRP2 differentiated autonomously into a uniform cell lineage displaying typical DC immunophenotypic markers. In agreement to our previous studies not conducted entirely under GMP but using similar methods, we detected approximately two LV copies per cell demonstrating comparable levels of gene transfer.[27] Detectable secretion of GM-CSF and IL-4 and two upregulated chemokines (monocyte chemoattractant protein-I and IL-8), which are all associated with DC differentiation/maturation/activation can be again attributed to specifications of SmartDC-TRP2 potency.[27] Thawed SmartDC-TRP2 cultured *in vitro* for 7 days stimulated autologous CTLs that could recognize and kill cell targets loaded with TRP2 antigens on the cell surface or expressing TRP2 endogenously.

One important concern for the *ex vivo* LV-based gene transfer is still safety. Although LVs were shown to be safe in clinical trials exploring gene transfer into hematopoietic stem cells and T cells,[25,43,47] monocytes genetically modified with LVs were never used clinically and there is a concern regarding insertional mutagenesis leading to myeloid malignancies. We therefore investigated the LV integration pattern in SmartDC-TRP2 by high-throughput IS analyses. Compared with the total sequences retrieved by the method, unique ISs in identifiable loci were reduced by 46-fold, possibly indicating a bottle-neck or integrations in previously non-annotated loci. As a hallmark of LV integration pattern, polyclonal integrated sequences were found downstream the transcription start site. The 10 most predominant clones did not show an integration bias for oncogenic loci. These results provide optimistic implications for the SmartDC-TRP2 cell vaccine and, further down, for a direct lentiviral vaccine bypassing *ex vivo* cell manipulations.

Incidentally, in parallel with the development of SmartDC-TRP2 for melanoma immunotherapy in the autologous setting, in recent years, our laboratory developed another type of engineered DC for use in the allogeneic transplantation setting. The target population are in this case immune-compromised cancer patients after allogeneic hematopoietic stem cell transplantation. The novel vaccine aspect is to accelerate the *de novo* donor-derived adaptive immune responses and protect the recipient against human cytomegalovirus (CMV). The vaccine consists of monocytes reprogrammed *ex vivo* with a tricistronic self-inactivating integrase defective LV (expressing GM-CSF, IFN-α and CMV-pp65 tegument protein) to allow direct generation of Self-differentiated Myeloid-derived Lentivirus-induced Dendritic Cells expressing pp65 (SmyleDCpp65). Our benchmark was to validate monocytes reprogrammed with integrase defective LV that self-differentiated into SmyleDCpp65 *in vitro* and *in vivo*.[48,49] SmyleDCpp65 promoted and accelerated *de novo* immune reconstitution of functional effector T and mature plasma B cells after $CD34^+$ peripheral blood hematopoietic stem cell transplantation in humanized NOD/$Rag1^{null}$/$IL2R\gamma^{null}$ (NRG) mice.[55] Remarkably, SmyleDCpp65 stimulated lymph node regeneration, thymopoiesis, human pp65-specific T-cell immunity and human antibody responses (immunoglobulin M and immunoglobulin G) in lymphopenic NRG transplanted mice. Xenograft Graft-versus-Host Disease (GvHD) was absent or mild, and no safety concerns were observed in this relevant animal model. Efficacy of cryopreserved/thawed SmyleDCpp65 was also established by extensive testing of pharmacodynamic activity in humanized mouse models. Feasibility of both integrase defective LV (ID-LV) production and GMP-compliant cell manufacturing were completed with a contract manufacturing organization (EUFETS GmbH, Germany; Sundarasetty *et al.,* submitted). Integrase defective LV are particularly attractive as their integration in the host genome is dramatically diminished (estimated to be 1000-fold), and thus resulting in lower risks of insertional mutagenesis.[50] Therefore, a next logical step to improve the SmartDC-TRP2 or lentiviral vaccine safety profile, will be to employ ID-LVs. Upon transduction of target cells, the default pathway of virus integration is changed

into accumulation of episomal circular viral genomes, whereby transgene expression still persists in differentiated DCs.

Ultimately, the future of lentivirus-reprogramming DCs performed *ex vivo* or *in vivo* is promising, as the cytokines and antigens used in the LV can be exchanged to suit the disease. This new methodology could modernize and transform the field of cancer vaccines. The method can potentially be entirely automatized for multicentric trials to answer questions of efficacy, aimed to promote multipotent cellular protection against specific antigens. The technology is modular and the applicability of this cell vaccine against cancer is broad, including further genetic engineering developments of the cell product as actively personalized vaccines, that is, by co-expression of tumor-specific neo-antigens.

MATERIALS AND METHODS

Cell lines

The HEK-293 (human embryonic kidney-293) cell line encoding the simian virus 40 large T antigen (heretofore, 293 T cells) was used for the production and characterization of LVs (both research grade and GMP grade). A fully characterized 293 T-based master cell bank was established at Cell and Gene Therapy at King's (King's College London, London, UK). FEMX-I (human malignant melanoma HLA-A*02:01 positive cell line, originating from a lymph node metastasis in a patient, kindly provided by Professor Dr. Udo Schumacher University Clinic Hamburg-Eppendorf) was used as targets in cytotoxicity assays. 293 T cells and FEMX-I cells were cultured at 37 °C and 5% CO_2 in Dulbecco's modified Eagle's medium (Invitrogen, Darmstadt, Germany) supplemented with 10% fetal bovine serum (HyClone, Bonn, Germany). K562 cells expressing HLA-A*02:01 (KA2 cells, kindly provided by Professor Dr. Thomas Woelfel, University Clinic Mainz) were transduced for TRP2 expression (KA2/TRP2) and cultured in RPMI supplemented with 10% fetal bovine serum, 1% Penicillin/Streptomycin and 1 mg ml^{-1} Geneticin (Biochrom AG, Berlin, Germany).

LVs and plasmids

LV-G24 (expressing human GM-CSF (hGM-CSF) and human IL-4) and LV-G242T (expressing, in addition, TRP2) were constructed and produced as described.[27,28] LV-G242T was produced under GMP conditions following standard operation procedure established at Cell and Gene Therapy at King's, King's College London. All packaging plasmids were fully sequenced and produced by PlasmidFactory GmbH (Bielefeld, Germany) as ccc-supercoiled plasmids, enzyme free and devoid of animal-derived materials and certified for purity. On day 0, multi-layer culture flasks were seeded with 293 T cells and cultured to sub-confluent optimal density in Dulbecco's modified Eagle's medium. $CaPO_4$ transfection was performed with the transfer plasmid and the packaging plasmids. 24 h after transfection, medium change and Benzonase treatment were performed. Supernatant containing virus was harvested at 24 h (harvest I) and 48 h (harvest II). The virus supernatant was first clarified through 0.45 µm filters and processed by anion exchange chromatography (CEX) using a MustangQ XT5 capsule (Pall). The column was sterilized with NaOH, and equilibrated with NaCl and Tris pH 8.0. Virus supernatant was adjusted to a final equimolar concentration of NaCl and Tris pH 8.0 and passed through the column. Virus particles were then eluted in increased NaCl/Tris pH 8.0 followed by phosphate-buffered saline (PBS). The eluate containing virus was then further diluted in PBS and subjected to centrifugation. After centrifugation, the virus was resuspended in CellGro medium (CellGenix, Freiburg, Germany). A 250-fold volume reduction was achieved from bulk harvest to final concentration. The CellGro formulated final concentrated virus suspension was filled in 1 ml per vial aliquots and stored at − 80 °C.

Titration of integrase defective LV-G2α2pp65 by p24 analyses

Physical titers of the vectors produced (research grade and GMP grade) were determined by quantifying the p24 HIV-I core protein by ELISA (QuickTiter HIV Lentivirus Quantitation Kit, BioCat, Heidelberg, Germany).

Titration of the vector and analyses of vector copy numbers in monocytes by RT-q-PCR

For virus titration, 293 T cells were transduced and genomic DNA was extracted from using the QiaAmp DNA blood mini kit (Qiagen, Hilden, Germany) according to the manufacturer's instructions. LV copy numbers were determined by real-time PCR as previously described.[49,51] Briefly, 2 µl containing 100 ng of genomic DNA were added to 13 µl of RT-q-PCR mix (containing 7.5 µl of SYBRTaq mix with 1 µl of wPRE/PTB2 primer mix (wPRE forward: 5′-GAGGAGTTGTGGCCCGTTGT-3′, wPRE reverse: 5′-TGACAGGTG GTGGCAATGCC-3′ or PTBP2 (polypyrimidine tract binding protein 2; PTBP2 forward: 5′-TCTCCATTCCCTATGTTCATGC-3′, PTBP2 reverse: 5′-GTTCCCGCAGAATGGTGAGGTG-3′) and 4.5 µl PCR grade, nuclease free water). All samples were analyzed with StepOnePlus Real time PCR system (Applied Biosystems, Life Technologies, Darmstadt, Germany). The cycling conditions were 10 min at 95 °C, 40 cycles of 15 s at 95 °C, 20 s at 56 °C and 30 s at 65 °C. Results were quantified by making use of primer pair-specific real-time PCR efficiencies and by comparing sample CT values with a standard curve generated with the plasmid vector (pCR4-TOPO) containing the wPRE and PTB2 sequences. Data was analyzed by StepOnePlus software (Applied Biosystems).

SmartDC-TRP2 generation from melanoma patients

Peripheral blood mononuclear cells were obtained as leukapheresis from melanoma patients in accordance with study protocols approved by Hannover Medical School Ethics Review Board. After informed consent, 50 cc peripheral blood mononuclear cell were collected at diagnosis from a total of 50 patients with melanoma stage III and IV. As some of our immune assays required antigen presentation through HLA-A*02:01, HLA typing was performed and we identified 20 patients. After a second informed consent, five HLA-A*02:01 melanoma patients (stage III and IV) who had reached remission and were stable were asked to donate additional leukapheresis material for more extensive immunologic assays, requiring large numbers of T cells. Tumor samples from three patients were confirmed to be positive for TRP2 expression by PCR.[52] SmartDC-TRP2 were generated from $CD14^+$ monocytes obtained from melanoma patients as previously described.[27] $CD14^+$ monocytes were isolated by immunomagnetic positive selection, (Miltenyi Biotec, Bergisch Gladbach, Germany) preconditioned with hGM-CSF and human IL-4 (50 ng ml^{-1} each, CellGenix) for 8 h. 2.5 µg ml^{-1} p24 equivalent of LV-G24 or LV-G242T were used to transduce 5×10^6 monocytes at multiplicity of infection (MOI) of 5 in the presence of 5 µg ml^{-1} protamine sulfate (Valeant, Eschborn, Germany) for 16 h. After transduction, cells were washed twice with CellGro medium (CellGenix). Conventional DCs (ConvDCs) were generated from monocytes by supplementing the medium with hGM-CSF and human IL-4 every 3 days.

Flow cytometry analyses of DCs

We used the following monoclonal antibodies reactive against DC markers: CD86-PE, HLA-DR-PerCP, CD80-PE, CCR2-AlexaFlour 647, CCR5-PerCP (Becton Dickinson, Heidelberg, Germany) and respective monoclonal antibody isotype controls. Cells were collected, washed once with PBS, blocked with PBS containing mouse IgG (50 µg ml^{-1}) incubated on ice for 15 min and stained with the corresponding monoclonal antibodies for 30 min. Cells were washed and resuspended in cell-fix solution (Becton Dickinson). Cells were then analyzed using a FACSCalibur cytometer (Becton Dickinson). Acquisition was performed using CellQuest software and analyses were performed using Flowjo software (Treestar Inc., Ashland, OR, USA).

Functional analyses of TRP2-specific T-cell responses in melanoma patients

SmartDC and SmartDC-TRP2 generated with peripheral blood mononuclear cells of melanoma patients were harvested 7 days after transduction and used directly for the first T-cell stimulations or cryopreserved for subsequent re-stimulations. Autologous $CD8^+$ T cells were selected from the $CD14^-$ fraction by magnetic bead isolation (Miltenyi Biotec). T cells and DCs were seeded at a 10:1 ratio (T:DC). Autologous feeder cells ($CD14^-$ /$CD8^-$) were gamma-irradiated with 40 Gy (Gammacell 3000 Elan, Best Theratronics Ltd., Ottawa, ON, Canada) and added to the co-cultures. Co-cultures were maintained for 7 days in X-VIVO-15 (Lonza, Köln, Germany) containing 5% human AB serum (Lonza, Basel, Switzerland) and cytokines IL-2: 25 infective unit per ml (Novartis

Pharma GmbH, Nürnberg, Germany), IL-7: 5 ng ml^{-1} and IL-15: 5 ng ml^{-1} (CellGenix). The medium with cytokines was replenished every 2 days. Re-stimulations were performed after every 7 days by adding the corresponding numbers of cryopreserved/thawed DCs, to the T cells at a ratio of T:DC of 10:1. Expanded T cells were analyzed by IFN-γ ELISPOT assay. 30 000 expanded T cells were harvested and seeded per well on IFN-γ antibody-coated ELISPOT plate and incubated overnight with KA2 cells, KA2 cells loaded with TRP2 overlapping peptide pool (KA2/peptide) or KA2 cells endogenously expressing TRP2 (KA2/TRP2). The plates were developed as described by the manufacturer (Mabtech, Nacka Strand, Sweden) and analyzed using ImmunoSpot Analyzer (CTL-Europe GmbH, Bonn, Germany).

Tetramer analysis of TRP2-reactive T cells

T cells expanded *in vitro* were stained with TRP2-specific tetramers: HLA-A*02:01-SVYDFFVWL-PE ($TRP2_{180\text{-}188}$) or HLA-A*02:01-TLDSQVMSL-APC ($TRP2_{360\text{-}368}$) produced at the Ludwig Institute for Cancer Research, Lausanne, Switzerland (kindly provided by Dr. Philippe Guillaume and Prof. Immanuel F. Luescher). An PE-conjugated irrelevant tetramer was used as negative control (Beckman Coulter, Krefeld, Germany). 2×10^5 stimulated T cells were incubated for 30 min at room temperature with tetramer, washed once, stained with surface antibodies (CD8-FITC, CD3-PECy7, BD Biosciences, Heidelberg, Germany) for 20 min at 4 °C, washed once, fixed and analyzed in a LSR II flow cytometer (BD Biosciences). At least 10 000 $CD3^+/CD8^+$ viable cells were analyzed. Tetramer-positive cells were expressed as the percentage of total $CD3^+/CD8^+$ T cells.

Carboxyfluorescein diacetate succinimidyl ester-based cytotoxicity analyses

Carboxyfluorescein diacetate succinimidyl ester (CFSE)-based cytotoxicity analyses were performed as described.[53] KA2/TRP2 or FEMX-I cells were washed with PBS, resuspended at 1×10^7 cells ml^{-1}, labeled with 10 μM CFSE (Sigma-Aldrich, Schnelldorf, Germany) for 10 min at 37 °C, washed and resuspended in X-VIVO-15 (Lonza) at 5×10^6 cells ml^{-1}. The T cells expanded with SmartDC or SmartDC-TRP2 cultures were harvested, washed and resuspended in X-VIVO-15 (Lonza) at 5×10^4 cells ml^{-1}. T cells and KA2/TRP2/CFSE or FEMX-I/CFSE targets were mixed in various E:T ratios and incubated at 37 °C and 5% CO_2 for 8 h. After co-culture, T cells were labeled with fluorochrome-conjugated antibodies (CD8-PE-Cy7 and CD3-APC; BD Biosciences). Fluorochrome-labeled microbeads were added to facilitate the quantification of the $CD3^-/CD8^-/CFSE^+$ not lysed melanoma cells by flow cytometry. The percentage-specific lysis was calculated by the following formula: % specific lysis = 100 – ($CD8^-CFSE^+$ live target cells in the test sample/$CD8^-CFSE^+$ live target cells in the control sample with no T cells) × 100. The acquisition was carried out in FACS LSR II (BD Biosciences) and the results were analyzed using Flowjo software v. 7.6.4 (Treestar Inc.).

SmartDC-TRP2 production under GMP-compliant conditions

After informed consent, leukapheresis was obtained from healthy adult volunteers (HLA-A*02:01) with a COBE Spectra apheresis system. $CD14^+$ monocytes were enriched by immunomagnetic separation using a GMP-compliant CliniMACS system (Miltenyi Biotec). Quantitative and qualitative analyses of the selected $CD14^+$ fraction and flow through were performed by flow cytometry. From the enriched $CD14^+$ fraction, 2×10^8 cells were resuspended in 25 ml of serum-free CellGro DC medium (CellGenix) and seeded in a 100 ml bag (CellGenix). Cells were preconditioned with 25 ml of medium containing hGM-CSF and human IL-4 cytokines (50 ng ml^{-1} each, CellGenix) for 8 h. Cells were transduced with 1×10^9 infective particles (multiplicity of infection of 5) in 50 ml medium containing Protamine sulfate (5 μg ml^{-1}). The bag was incubated at 37 °C and 5% CO_2 for 16 h. Next day, cells were washed three times with CellGro medium. After washing, cell number and viability was determined. Transduced cells were cryopreserved in aliquots of 2×10^6 cell ml^{-1} per vial. Surplus, non-transduced monocytes were cryopreserved in aliquots of 2×10^6 cell ml^{-1} per vial and 50×10^6 cell ml^{-1} per vial and were used as controls for the characterization experiments. Sterility tests were performed with the 'Bactec' system (BD Biosciences).

Analyses of thawed GMP-grade SmartDC-TRP2 by flow cytometry analyses

Monocytes transduced with LV-G242T were seeded at a concentration of $1x10^6$ cells ml^{-1} in CellGro and analyzed after 1, 3 or 7 days of *in vitro* culture. Surface marker expression was analyzed by flow cytometry using the following monoclonal antibody conjugated with fluorochromes: CD209-FITC, CD14-PE, HLA-DR-PerCP and CD86-APC (BD Biosciences). Non-transduced monocytes were used as negative controls and conventional DCs (ConvDCs) were used as positive controls. Acquisitions and analyses were performed by LSR II and Flowjo analyses software.

Analyses of cytokines and transgene expression

Cytokines accumulated in SmartDC-TRP2 culture supernatants were analyzed by multiplex luminex based kit according to the manufacturer's protocol (Milliplex Millipore, MA, USA).

Analyses of GMP-grade SmartDC-TRP2 potency by T-cell stimulation *in vitro*

$CD3^+$ T cells autologous to DCs were isolated from the $CD14^-$ fraction by magnetic-activated cell sorting-positive selection (MACS, Miltenyi Biotec). IFN-γ ELISPOT with the stimulated T cells was performed as described above. Non-radioactive and colorimetric based cytotoxicity assays were performed with CytoTox 96 non-radioactive cytotoxicity assay (Promega, Mannheim, Germany) according to the manufacturer's protocol. $CD8^+$ T cells were stimulated with SmartDC or SmartDC/pep or SmartDC-TRP2 and subsequently were co-cultured with 10 000 KA2/TRP2 cells per well at various E:T ratios. Target cell lysis was measured by quantifying lactate dehydrogenase release into the medium in an enzymatic coupled assay. Percentage cytotoxicity was calculated by the following formula: % Cytotoxicity = (Experimental release – Effector spontaneous – Target spontaneous/Target maximum – Target spontaneous) × 100. Graphs depict the values quantified from triplicate wells.

Integration analyses by next-generation sequencing

Integration analyses were performed using LAM-PCR to identify the LV-flanking genomic sequences as described.[31] Briefly, total DNA was extracted from the samples after 7 days in culture as described.[54] Two 50-cycle linear PCR amplification steps were carried out using biotinylated primers hybridizing to the 3-prime region of the long-terminal repeats of the vector. The biotinylated PCR products were further captured with paramagnetic beads followed by second strand DNA synthesis, restriction digestion and ligation of a cohesive double-stranded linker sequence carrying a molecular barcode of 12 nucleotides. Two nested PCR were then performed with linker- and vector-specific primers each complementary to one of the known ends of the target DNA. In 5′–3′ orientation, LAM-PCR products contained a long-terminal repeat sequence, a flanking human genomic sequence and a linker cassette sequence. LAM-PCR amplicons were further prepared for MiSeq sequencing (Illumina, San Diego, CA, USA). Therefore, an additional PCR with special fusion primers carrying MiSeq-specific sequencing adapters was performed. DNA barcoding was used to allow parallel sequencing of multiple samples in a single sequencing run. Libraries were mixed with an φX bacteriophage genome library to introduce diversity and optimize the sequencing run performance and sequenced using the Illumina MiSeq v2 Reagent Kit. The pair-end runs were initiated for Illunima's sequencing by synthesis technology, including clustering, paired-end preparation, barcode sequencing and analysis. After completion of the run, base calling was performed on data, sequences were de-multiplexed and φX reads were filtered. Next-generation sequencing data processing dealt with the management of high-throughput data from Roche 454/Illumina MiSeq sequencing platforms and comprise two main goals: (1) data quality inspection and analysis, in which LV sequences and other contaminants were trimmed; (2) integration site identification, in which all valid sequence reads are aligned to the genome of reference and valid ISs were retrieved.

Statistical analysis

Student's *t*-tests and Bonferroni post-tests were performed for the data derived using the GraphPad Prism software (GraphPad Software Inc., La Jolla, CA, USA). All tests were two-sided and the *P*-values < 0.05 were considered significant and were indicated.

CONFLICT OF INTEREST

The authors declare no conflict of interest.

ACKNOWLEDGEMENTS

We thank all past members of the UCLA Vector Core and the MHH Regenerative Immune Therapies Applied Group for their previous contributions to this project, in special Dr Richard Koya and Dr Mudita Pincha. We thank the staff of the Department of Dermatology of the MHH for their assistance in procuring samples and leukapheresis from melanoma patients. We thank the staff of the Institute of Transfusion Medicine (Dr Lilia Goudeva, Stephanie Vahlsing and Marina Kramer) for procurement of leukapheresis from healthy donors and technical assistance with some immune assays. Many thanks to Philippe Guillaume and Immanuel F Luescher from the Lausanne Tetramer Core facility, Ludwig Institute for Cancer Research (Lausanne, Switzerland) for kindly providing us with the tetramers against TRP2. We thank Professor Dr Udo Schumacher University Clinic Hamburg-Eppendorf, Germany for providing us with the HLA-A*02:01 positive FEMX-I human malignant melanoma cell line. We thank Prof. Heiko von der Leyen and his staff of the Hannover Clinical Trial Center for supporting the scientific advice meetings and discussions with the German regulatory agencies for future clinical trials employing SmartDC-TRP2. This work was supported by grants of the German Research Council (DFG/ Excellence Cluster REBIRTH to RS and CF) and Deutsche Krebshilfe (to RS and RG).

REFERENCES

1 Flaherty KT, Hodi FS, Fisher DE. From genes to drugs: targeted strategies for melanoma. *Nat Rev Cancer* 2012; **12**: 349–361.
2 Eggermont AM, Robert C. New drugs in melanoma: it's a whole new world. *Eur J Cancer* 2011; **47**: 2150–2157.
3 Hauschild A, Grob JJ, Demidov LV, Jouary T, Gutzmer R, Millward M *et al.* Dabrafenib in BRAF-mutated metastatic melanoma: a multicentre, open-label, phase 3 randomised controlled trial. *Lancet* 2012; **380**: 358–365.
4 Sosman JA, Kim KB, Schuchter L, Gonzalez R, Pavlick AC, Weber JS *et al.* Survival in BRAF V600-mutant advanced melanoma treated with vemurafenib. *N Engl J Med* 2012; **366**: 707–714.
5 Hodi FS, O'Day SJ, McDermott DF, Weber RW, Sosman JA, Haanen JB *et al.* Improved survival with ipilimumab in patients with metastatic melanoma. *N Engl J Med* 2010; **363**: 711–723.
6 Voskens CJ, Goldinger SM, Loquai C, Robert C, Kaehler KC, Berking C *et al.* The price of tumor control: an analysis of rare side effects of anti-CTLA-4 therapy in metastatic melanoma from the ipilimumab network. *PLoS One* 2013; **8**: e53745.
7 Hamid O, Robert C, Daud A, Hodi FS, Hwu WJ, Kefford R *et al.* Safety and tumor responses with lambrolizumab (anti-PD-1) in melanoma. *N Engl J Med* 2013; **369**: 134–144.
8 Robert C, Ribas A, Wolchok JD, Hodi FS, Hamid O, Kefford R *et al.* Anti-programmed-death-receptor-1 treatment with pembrolizumab in ipilimumab-refractory advanced melanoma: a randomised dose-comparison cohort of a phase 1 trial. *Lancet* 2014; **384**: 1109–1117.
9 Robert C, Long GV, Brady B, Dutriaux C, Maio M, Mortier L *et al.* Nivolumab in previously untreated melanoma without BRAF mutation. *N Engl J Med* 2015; **372**: 320–330.
10 Hinrichs CS, Rosenberg SA. Exploiting the curative potential of adoptive T-cell therapy for cancer. *Immunological reviews* 2014; **257**: 56–71.
11 Ott PA, Fritsch EF, Wu CJ, Dranoff G. Vaccines and melanoma. *Hematol Oncol Clin North Am* 2014; **28**: 559–569.
12 Engell-Noerregaard L, Hansen TH, Andersen MH, Thor Straten P, Svane IM. Review of clinical studies on dendritic cell-based vaccination of patients with malignant melanoma: assessment of correlation between clinical response and vaccine parameters. *Cancer Immunol Immunother* 2009; **58**: 1–14.
13 De Vries IJ, Krooshoop DJ, Scharenborg NM, Lesterhuis WJ, Diepstra JH, Van Muijen GN *et al.* Effective migration of antigen-pulsed dendritic cells to lymph nodes in melanoma patients is determined by their maturation state. *Cancer Res* 2003; **63**: 12–17.
14 Schadendorf D, Ugurel S, Schuler-Thurner B, Nestle FO, Enk A, Brocker EB *et al.* Dacarbazine (DTIC) versus vaccination with autologous peptide-pulsed dendritic cells (DC) in first-line treatment of patients with metastatic melanoma: a randomized phase III trial of the DC study group of the DeCOG. *Ann Oncol* 2006; **17**: 563–570.
15 Lopez MN, Pereda C, Segal G, Munoz L, Aguilera R, Gonzalez FE *et al.* Prolonged survival of dendritic cell-vaccinated melanoma patients correlates with tumor-specific delayed type IV hypersensitivity response and reduction of tumor growth factor beta-expressing T cells. *J Clin Oncol* 2009; **27**: 945–952.
16 Steele JC, Rao A, Marsden JR, Armstrong CJ, Berhane S, Billingham LJ *et al.* Phase I/II trial of a dendritic cell vaccine transfected with DNA encoding melan A and gp100 for patients with metastatic melanoma. *Gene Ther* 2011; **18**: 584–593.
17 Kyte JA, Kvalheim G, Lislerud K, thor Straten P, Dueland S, Aamdal S *et al.* T cell responses in melanoma patients after vaccination with tumor-mRNA transfected dendritic cells. *Cancer Immunol Immunother* 2007; **56**: 659–675.
18 Wilgenhof S, Van Nuffel AM, Benteyn D, Corthals J, Aerts C, Heirman C *et al.* A phase IB study on intravenous synthetic mRNA electroporated dendritic cell immunotherapy in pretreated advanced melanoma patients. *Ann Oncol* 2013; **24**: 2686–2693.
19 Wilgenhof S, Corthals J, Van Nuffel AM, Benteyn D, Heirman C, Bonehill A *et al.* Long-term clinical outcome of melanoma patients treated with messenger RNA-electroporated dendritic cell therapy following complete resection of metastases. *Cancer Immunol Immunother* 2015; **64**: 381–388.
20 Ribas A. Genetically modified dendritic cells for cancer immunotherapy. *Curr Gene Ther* 2005; **5**: 619–628.
21 Dullaers M, Breckpot K, Van Meirvenne S, Bonehill A, Tuyaerts S, Michiels A *et al.* Side-by-side comparison of lentivirally transduced and mRNA-electroporated dendritic cells: implications for cancer immunotherapy protocols. *Mol Ther* 2004; **10**: 768–779.
22 Pincha M, Sundarasetty BS, Stripecke R. Lentiviral vectors for immunization: an inflammatory field. *Expert Rev Vaccines* 2010; **9**: 309–321.
23 Porter DL, Levine BL, Kalos M, Bagg A, June CH. Chimeric antigen zreceptor-modified T cells in chronic lymphoid leukemia. *N Engl J Med* 2011; **365**: 725–733.
24 Biffi A, Bartolomae CC, Cesana D, Cartier N, Aubourg P, Ranzani M *et al.* Lentiviral vector common integration sites in preclinical models and a clinical trial reflect a benign integration bias and not oncogenic selection. *Blood* 2011; **117**: 5332–5339.
25 Aiuti A, Biasco L, Scaramuzza S, Ferrua F, Cicalese MP, Baricordi C *et al.* Lentiviral hematopoietic stem cell gene therapy in patients with Wiskott-Aldrich syndrome. *Science* 2013; **341**: 1233151.
26 Koya RC, Kimura T, Ribas A, Rozengurt N, Lawson GW, Faure-Kumar E *et al.* Lentiviral vector-mediated autonomous differentiation of mouse bone marrow cells into immunologically potent dendritic cell vaccines. *Mol Ther* 2007; **15**: 971–980.
27 Pincha M, Sundarasetty BS, Salguero G, Gutzmer R, Garritsen H, Macke L *et al.* Identity, potency, in vivo viability, and scaling up production of lentiviral vector-induced dendritic cells for melanoma immunotherapy. *Hum Gene Ther Methods* 2012; **23**: 38–55.
28 Salguero G, Sundarasetty BS, Borchers S, Wedekind D, Eiz-Vesper B, Velaga S *et al.* Preconditioning therapy with lentiviral vector-programmed dendritic cells accelerates the homeostatic expansion of antigen-reactive human T cells in NOD. Rag1($^{-/-}$).IL-2rgammac($^{-/-}$) mice. *Hum Gene Ther* 2011; **22**: 1209–1224.
29 Pincha M, Salguero G, Wedekind D, Sundarasetty BS, Lin A, Kasahara N *et al.* Lentiviral vectors for induction of self-differentiation and conditional ablation of dendritic cells. *Gene Ther* 2011; **18**: 750–764.
30 Wang RF, Appella E, Kawakami Y, Kang X, Rosenberg SA. Identification of TRP-2 as a human tumor antigen recognized by cytotoxic T lymphocytes. *J Exp Med* 1996; **184**: 2207–2216.
31 Schmidt M, Schwarzwaelder K, Bartholomae C, Zaoui K, Ball C, Pilz I *et al.* High-resolution insertion-site analysis by linear amplification-mediated PCR (LAM-PCR). *Nat Methods* 2007; **4**: 1051–1057.
32 Cattoglio C, Facchini G, Sartori D, Antonelli A, Miccio A, Cassani B *et al.* Hot spots of retroviral integration in human CD34+ hematopoietic cells. *Blood* 2007; **110**: 1770–1778.
33 Pak BJ, Lee J, Thai BL, Fuchs SY, Shaked Y, Ronai Z *et al.* Radiation resistance of human melanoma analysed by retroviral insertional mutagenesis reveals a possible role for dopachrome tautomerase. *Oncogene* 2004; **23**: 30–38.
34 Boasberg PD, Hoon DS, Piro LD, Martin MA, Fujimoto A, Kristedja TS *et al.* Enhanced survival associated with vitiligo expression during maintenance biotherapy for metastatic melanoma. *J Invest Dermatol* 2006; **126**: 2658–2663.
35 Khong HT, Rosenberg SA. Pre-existing immunity to tyrosinase-related protein (TRP)-2, a new TRP-2 isoform, and the NY-ESO-1 melanoma antigen in a patient with a dramatic response to immunotherapy. *J Immunol* 2002; **168**: 951–956.
36 Paschen A, Song M, Osen W, Nguyen XD, Mueller-Berghaus J, Fink D *et al.* Detection of spontaneous CD4+ T-cell responses in melanoma patients against a tyrosinase-related protein-2-derived epitope identified in HLA-DRB1*0301 transgenic mice. *Clin Cancer Res* 2005; **11**: 5241–5247.
37 Umansky V, Abschuetz O, Osen W, Ramacher M, Zhao F, Kato M *et al.* Melanoma-specific memory T cells are functionally active in Ret transgenic mice without macroscopic tumors. *Cancer Res* 2008; **68**: 9451–9458.
38 Eyles J, Puaux AL, Wang X, Toh B, Prakash C, Hong M *et al.* Tumor cells disseminate early, but immunosurveillance limits metastatic outgrowth, in a mouse model of melanoma. *J Clin Invest* 2010; **120**: 2030–2039.
39 Kuo CT, Hoon DS, Takeuchi H, Turner R, Wang HJ, Morton DL *et al.* Prediction of disease outcome in melanoma patients by molecular analysis of paraffin-embedded sentinel lymph nodes. *J Clin Oncol* 2003; **21**: 3566–3572.

40 Takeuchi H, Kuo C, Morton DL, Wang HJ, Hoon DS. Expression of differentiation melanoma-associated antigen genes is associated with favorable disease outcome in advanced-stage melanomas. *Cancer Res* 2003; **63**: 441–448.
41 Tumeh PC, Harview CL, Yearley JH, Shintaku IP, Taylor EJ, Robert L *et al.* PD-1 blockade induces responses by inhibiting adaptive immune resistance. *Nature* 2014; **515**: 568–571.
42 Linnemann C, van Buuren MM, Bies L, Verdegaal EM, Schotte R, Calis JJ *et al.* High-throughput epitope discovery reveals frequent recognition of neo-antigens by CD4+ T cells in human melanoma. *Nat Med* 2015; **21**: 81–85.
43 Biffi A, Montini E, Lorioli L, Cesani M, Fumagalli F, Plati T *et al.* Lentiviral hematopoietic stem cell gene therapy benefits metachromatic leukodystrophy. *Science* 2013; **341**: 1233158.
44 Merten OW, Charrier S, Laroudie N, Fauchille S, Dugue C, Jenny C *et al.* Large-scale manufacture and characterization of a lentiviral vector produced for clinical *ex vivo* gene therapy application. *Hum Gene Ther* 2011; **22**: 343–356.
45 Oshita C, Takikawa M, Kume A, Miyata H, Ashizawa T, Iizuka A *et al.* Dendritic cell-based vaccination in metastatic melanoma patients: phase II clinical trial. *Oncol Rep* 2012; **28**: 1131–1138.
46 Ellebaek E, Engell-Noerregaard L, Iversen TZ, Froesig TM, Munir S, Hadrup SR *et al.* Metastatic melanoma patients treated with dendritic cell vaccination, Interleukin-2 and metronomic cyclophosphamide: results from a phase II trial. *Cancer Immunol Immunother* 2012; **61**: 1791–1804.
47 Grupp SA, Kalos M, Barrett D, Aplenc R, Porter DL, Rheingold SR *et al.* Chimeric antigen receptor-modified T cells for acute lymphoid leukemia. *N Engl J Med* 2013; **368**: 1509–1518.
48 Daenthanasanmak A, Salguero G, Borchers S, Figueiredo C, Jacobs R, Sundarasetty BS *et al.* Integrase-defective lentiviral vectors encoding cytokines induce differentiation of human dendritic cells and stimulate multivalent immune responses *in vitro* and *in vivo*. *Vaccine* 2012; **30**: 5118–5131.
49 Salguero G, Daenthanasanmak A, Munz C, Raykova A, Guzman CA, Riese P *et al.* Dendritic cell-mediated immune humanization of mice: implications for allogeneic and xenogeneic stem cell transplantation. *J Immunol* 2014; **192**: 4636–4647.
50 Yanez-Munoz RJ, Balaggan KS, MacNeil A, Howe SJ, Schmidt M, Smith AJ *et al.* Effective gene therapy with nonintegrating lentiviral vectors. *Nat Med* 2006; **12**: 348–353.
51 Rothe M, Rittelmeyer I, Iken M, Rudrich U, Schambach A, Glage S *et al.* Epidermal growth factor improves lentivirus vector gene transfer into primary mouse hepatocytes. *Gene Ther* 2012; **19**: 425–434.
52 Sarantou T, Chi DD, Garrison DA, Conrad AJ, Schmid P, Morton DL *et al.* Melanoma-associated antigens as messenger RNA detection markers for melanoma. *Cancer research* 1997; **57**: 1371–1376.
53 Sundarasetty BS, Singh VK, Salguero G, Geffers R, Rickmann M, Macke L *et al.* Lentivirus-induced dendritic cells for immunization against high-risk WT1(+) acute myeloid leukemia. *Hum Gene Ther* 2013; **24**: 220–237.
54 Badralmaa Y, Natarajan V. Impact of the DNA extraction method on 2-LTR DNA circle recovery from HIV-1 infected cells. *J Virol Methods* 2013; **193**: 184–189.
55 Daenthanasanmak A, Salguero G, Sundarasetty BS, Waskow C, Cosgun KN, Guzman C A *et al.* Engineered dendritic cells from cord blood and adult blood accelerate effector T cell immune reconstitution against HCMV. *Mol Ther Methods Clin Dev* 2014; **1**: 14060.